Fission fragment mass distributions in reactions forming the ^{213}Fr compound nucleus

S. Appannababu,[1,*] S. Mukherjee,[1] B. K. Nayak,[2] R. G. Thomas,[2] P. Sugathan,[3] A. Jhingan,[3] E. Prasad,[4] D. Negi,[3] N. N. Deshmukh,[1] P. K. Rath,[1] N. L. Singh,[1] and R. K. Choudhury[2]

[1]*Department of Physics, Faculty of Science, The M. S. University of Baroda, Vadodara 390002, India*

[2]*Nuclear Physics Division, Bhabha Atomic Research Centre, Mumbai 400085, India*

[3]*Inter-University Accelerator Centre, Aruna Asaf Ali Marg, New Delhi 110067, India*

[4]*Department of Physics, Calicut University, Calicut 673635, India*

(Received 1 September 2010; published 10 March 2011)

The fission fragment mass angle correlations and mass ratio distributions have been investigated for the two systems ^{16}O + ^{197}Au and ^{27}Al + ^{186}W, leading to the same compound nucleus ^{213}Fr around the Coulomb barrier energies. Systematic analysis of the variance of the mass distributions as a function of temperature and angular momentum suggests true compound nuclear fission for both the reactions, indicating the absence of nonequilibrium fission processes.

DOI: 10.1103/PhysRevC.83.034605 PACS number(s): 25.70.Jj, 25.85.Ge, 25.70.Gh, 27.90.+b

I. INTRODUCTION

Recently there has been much progress in the study of fusion-fission reactions with less fissile medium mass nuclei to investigate the factors that lead to the hindrance in compound nucleus (CN) formation [1–3]. The CN formation is strongly reduced around the fusion barrier energies due to the presence of a nonequilibrium process called quasifission (QF) [4,5]. In this process the interacting system reseparates before reaching a compact or definite CN shape. Due to the presence of the QF process, fission fragment anisotropies have been observed to be anomalous in comparison to standard statistical model predictions and also the fission fragment mass widths have been observed to be large in comparison to the CN events. The competition between QF and CN formation determines the survival probability of evaporation residues, which is important in understanding the fusion-fission dynamics for the production of heavy and superheavy elements. It is well known that the entrance channel properties, such as the mass asymmetry (α) of the interacting systems with respect to the Businaro-Gallone mass asymmetry ($\alpha_{\rm BG}$), the static deformation, and the product of Z_pZ_t of the interacting systems, play an important role in the formation of the CN. The entrance mass asymmetry of the interacting projectile-target combinations decides the direction of the mass flow in the dinuclear system. Earlier dynamical models predicted that QF occurs when $Z_pZ_t \geqslant 1600$ [4] (where Z_p and Z_t are the projectile and target atomic numbers, respectively) but recent results show that the onset of QF starts at a Z_pZ_t value equal to nearly 1000 and plays a dominant role at higher values of Z_pZ_t [1]. It is also reported that with deformed targets/projectiles the nuclear orientation of the interacting nuclei and shell effects play a major role in the survival probability of the CN [6,7]. One can infer the occurrence of QF by measuring the evaporation residue (ER) cross sections, fission fragment angular distributions and mass distributions.

Earlier experimental evidence of QF was observed with projectiles $A \geqslant 24$ through fission fragment angular distribution studies [8], where the experimental anisotropies are much larger than the standard statistical saddle point theoretical model predictions. But recently there is evidence of QF with less asymmetric systems like ^{19}F + ^{197}Au [3]. The observation of QF with less asymmetric reactions has been attributed to the entrance channel properties of the interacting systems in which the entrance channel mass asymmetry (α) is smaller than the critical Businaro-Gallone mass asymmetry ($\alpha_{\rm BG}$) [9]. The study of fusion-fission dynamics in the medium mass region $A \approx 200$–220 is very interesting due to the observation of many unexpected results, even though the reactions studied have similar Z_pZ_t values. For example, the fusion-fission process in the CN Ra was of great interest due to the observation of reduced ER cross sections and large mass angle correlations with different entrance channels. In the past, the suppression of ER cross sections have been reported due to the presence of QF for ^{22}Ne + ^{194,196,198}Pt and ^{48}Ca + ^{168,170}Er systems [10]. In another work, evidence of shell effects in the fission fragment mass distribution has been found in the ^{48}Ca +^{168}Er reaction, where a contribution of 30% of asymmetric fission in the total fusion-fission reaction has been reported [7]. The same CN was studied by measuring ER cross sections and fission mass angle correlations by different entrance channels [3]. Strong evidence of QF was found in the less asymmetric system ^{19}F + ^{197}Au ($Z_pZ_t = 711$) [3]. But no evidence for QF was observed in the investigation of fission fragment angular distributions as the experimental results were matching with theoretical predictions for CN fission [11].

Earlier, it was shown that QF starts at around $Z_pZ_t = 1000$ and plays a dominant role around $Z_pZ_t = 1400$ [1]. However, recent results show strong evidence of QF in the reactions with $Z_pZ_t$values around 900 [12]. The compound system Fr is very close to Ra and the Z_pZ_t values of the present studied systems are similar to the previously reported ones, where reduction in evaporation residue cross sections and broader mass angle correlations have been reported. Therefore, it is of interest to investigate mass angle correlations and fission fragment angular distributions in the case of the Fr compound

*babu.msu@gmail.com

TABLE I. Entrance channel parameters of the various systems studied.

Systems studied	V_B (MeV)	Z_pZ_t	α
$^{16}O + ^{197}Au$	74.84	632	0.849
$^{27}Al + ^{186}W$	110.91	962	0.746

system to study the contribution of QF in the above systems. Earlier we reported fission fragment angular distributions for $^{11}B + ^{204}Pb$ and $^{18}O + ^{197}Au$ systems leading to the same CN ^{215}Fr [13]. There is no evidence of QF for the system $^{18}O + ^{197}Au$ even though it is having entrance channel mass asymmetry very much similar to $^{19}F + ^{197}Au$. In this context the main objective of the present work is to understand the mass relaxation mechanism in less fissile systems and the contribution, if any, of the QF process. We have measured the fission mass angle correlations for the CN ^{213}Fr populated through two different reactions $^{16}O + ^{197}Au$ ($Z_pZ_T = 632$) and $^{27}Al + ^{186}W$ ($Z_pZ_T = 962$) around the Coulomb barrier energies.

II. EXPERIMENTAL PROCEDURE

The experiment was performed by using the 15 UD pelletron accelerator facility at the Inter-University Accelerator Centre (IUAC), New Delhi, India, in a 1.5-m-diameter general purpose scattering chamber (GPSC). Beams of ^{16}O and ^{27}Al were bombarded on a self-supporting ^{197}Au target of thickness 150 $\mu g/cm^2$ and a highly enriched ^{186}W (99.5%) target of thickness 110 $\mu g/cm^2$ on 15 $\mu g/cm^2$ carbon backing, respectively. The measurements were carried out at a laboratory beam energy range of 79–100 MeV for $^{16}O + ^{197}Au$ and 123–140 MeV for $^{27}Al + ^{186}W$, respectively. Table I gives the entrance channel parameters of the systems studied in the present work. The beam energies were corrected for the energy loss in the half thickness of the targets. The schematic diagram of the experimental setup used for detecting fission fragments is shown in Fig. 1. Two large area (20.0 cm × 10.0 cm) position-sensitive multiwire proportional counters (MWPC) [14] were placed at a distance of 40.0 and 55.0 cm, respectively,

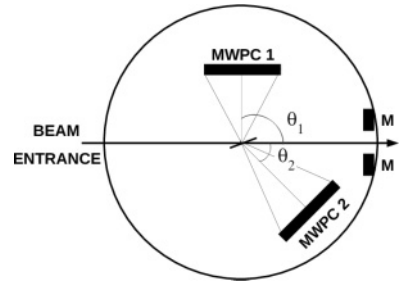

FIG. 1. Schematic experimental setup for measuring mass angle correlations.

from the target, on rotatable arms inside the scattering chamber to detect the fission fragments. These two MWPCs were kept at folding angles to detect the complementary fission fragments in coincidence. The two detectors were operated at a gas pressure of 3.0 mb of isobutane gas. Two Si surface barrier detectors were placed at ±10 degrees with respect to the beam direction at a distance of 70.0 cm from the target. These detectors were used to measure the elastically scattered beam particles and to monitor the position of the beam on the target. The time difference method was employed to extract the mass angle correlations using dc beams. It is well known that the time difference method is valid only when the targets used in the reactions are nonfissile, when transfer-induced fission is negligibly small, and strictly only when a binary reaction is taking place [15]. The above-mentioned properties are valid for the present reactions studied. The fission is expected from only full momentum transfer in these reactions; hence the time difference method can be applied. The gas detectors provided a position resolution of better than 1.5 mm. The position information of the fission fragments entering the detectors was obtained from the delay line readout of the MWPC wire planes. The central foil of both the MWPCs recorded the timing and energy loss signals. Each event at the position (x, y) on the active area of the detectors was transformed to give the scattering angles (θ, ϕ) with respect to the beam axis. The solid angle of both the gas detectors was determined online by taking elastic scattering data in singles mode below the Coulomb barrier and by using a fission source (^{252}Cf) of known strength in offline mode. The time difference information was obtained

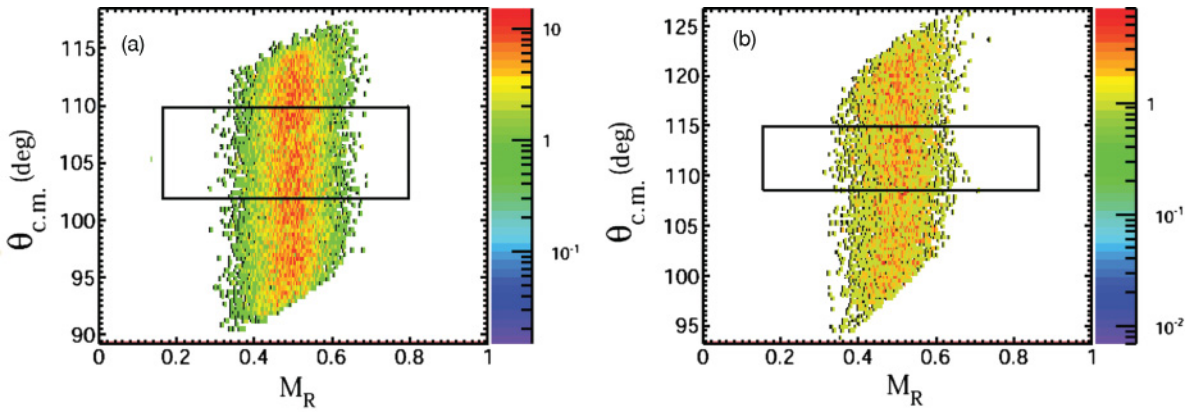

FIG. 2. (Color online) The mass ratio vs center of mass angle density plots for (a) $^{16}O + ^{197}Au$ and (b) $^{27}Al + ^{186}W$ at $E_{c.m.}/V_B = 0.97$.

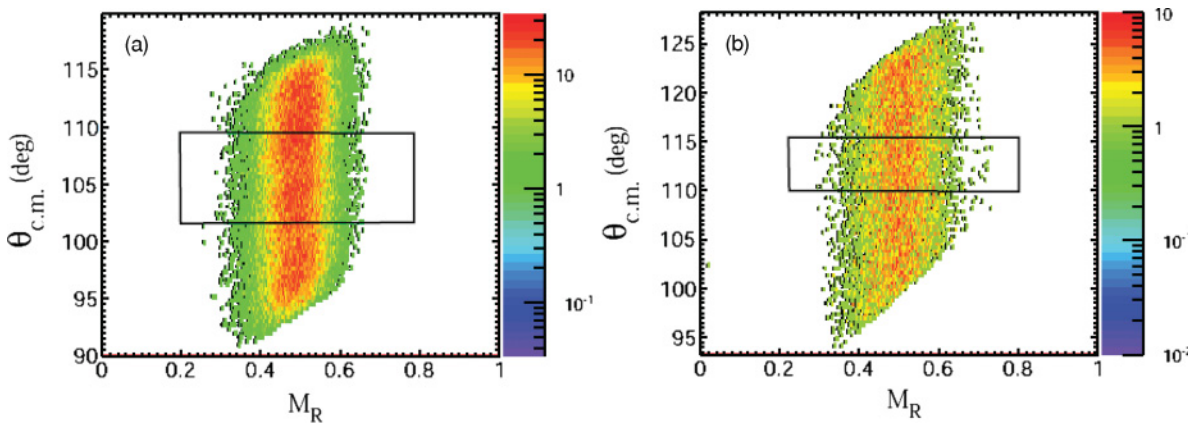

FIG. 3. (Color online) The mass ratio vs center of mass angle density plots for (a) $^{16}O + ^{197}Au$ and (b) $^{27}Al + ^{186}W$ at $E_{c.m.}/V_B = 1$.

by taking the start signal from the anode of the back detector and the stop signal from the anode of the front detector after delay. The masses of the fission fragments were reconstructed by using the (θ, ϕ) and the time difference information. The time difference information between the two fission fragments entering the two detectors was obtained in the following way:

$$t_1 - t_2 = \frac{d_1}{v_1} - \frac{d_2}{v_2} = \frac{d_1 m_1}{p_1} - \frac{d_2}{p_2}(m_{CN} - m_1), \qquad (1)$$

where m_{CN} is the mass of the fissioning CN, d_1 and d_2 are the flight paths of the fission fragments having masses m_1 and m_2, and p_1 and p_2 are the momenta of the fission fragments, which can be obtained by application of proper kinematic transformations and conservation of linear momentum. Further the above equation can be simplified to obtain the masses of the fission fragments as

$$m_1 = \frac{(t_1 - t_2) + \delta t_0 + m_{CN}\frac{d_2}{p_2}}{\frac{d_1}{p_1} + \frac{d_2}{p_2}}, \qquad (2)$$

and $m_2 = m_{CN} - m_1$.

Here δt_0 is the electronic delay between the timing signals of the two MWPCs, which can be obtained by imposing the condition that the mass ratio distribution is reflection symmetric at about 0.5 at $\theta_{c.m.} = 90^\circ$ for the reaction $^{16}O + ^{197}Au$, which is expected to fission through true CN formation.

The mass ratio (M_R) was obtained by using the following relation [2]:

$$M_R = \frac{m_2}{m_1 + m_2}. \qquad (3)$$

III. RESULTS AND DISCUSSION

The experimentally extracted mass angle correlations for the two systems $^{16}O + ^{197}Au$ and $^{27}Al + ^{186}W$ at $E_{c.m.}/V_B = 0.97$, 1.0, and 1.1 are shown in Figs. 2– 4 where the center of mass angle has been plotted against the mass ratios. Mass ratio spectra were generated by imposing rectangular gates as shown in the Fig. 2. The region inside the rectangular gate was only used to generate the mass ratio spectrum, to avoid any biasing due to the geometrical limitations of the experimental setup. The mass ratio spectra for both the systems at different energies are shown in Figs. 5 and 6. The experimental mass ratio distributions in Figs. 5 and 6 show no significant dependence of mass ratio on the center of mass angle. It can be observed that the mass ratio distributions are well described by Gaussians centered at $M_R = 0.5$ at all the energies. It is known that the σ_M^2 depends on the excitation energy and the fission mean square angular momentum of the CN by assuming that all the reactions go to fission through CN formation. This can be

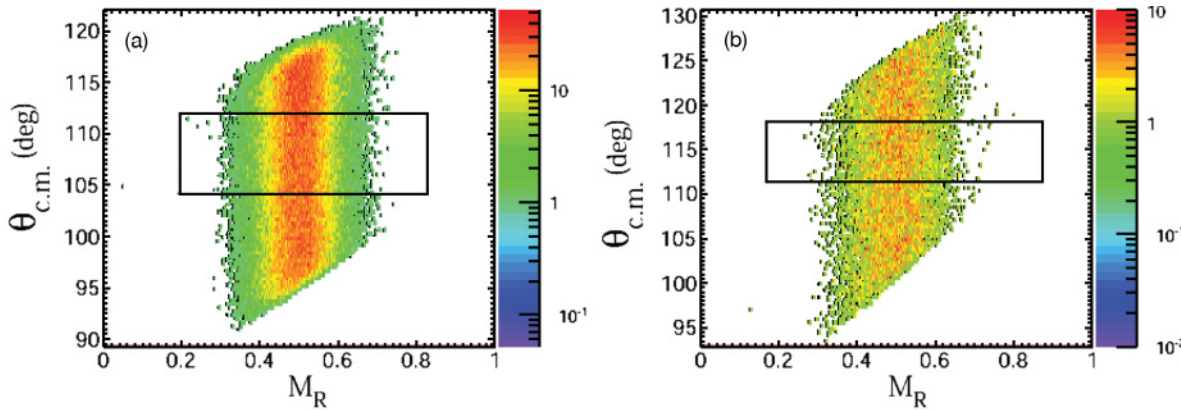

FIG. 4. (Color online) The mass ratio vs center of mass angle density plots for (a) $^{16}O + ^{197}Au$ and (b) $^{27}Al + ^{186}W$ at $E_{c.m.}/V_B = 1.1$.

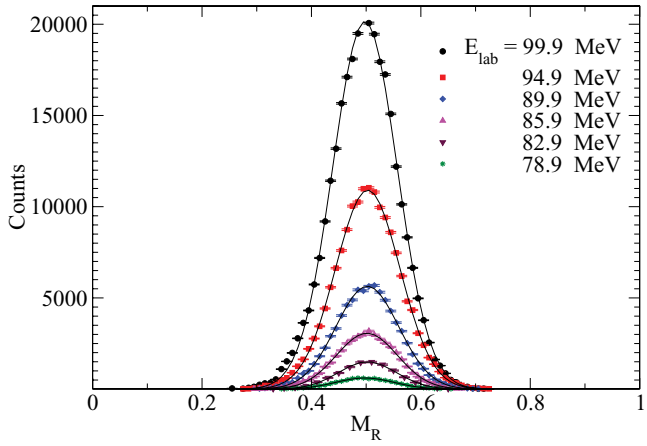

FIG. 5. (Color online) Mass ratio distributions for the reaction $^{16}O + ^{197}Au$ at different bombarding energies along with the Gaussian fits.

expressed by the relation $\sigma_M^2 = \nu T + \mu\langle l^2\rangle$, where ν and μ are fitting parameters, T is the average temperature, and $\langle l^2\rangle$ is the mean square angular momentum of the fissioning nucleus [16]. The l^2 values are calculated by reproducing the fusion excitation functions for $^{16}O + ^{197}Au$ [10] by using coupled channels code CCFULL [17]. The deformation parameters for the target/projectile nuclei were taken from the literature [18]. The temperature of the fissioning CN at the saddle point can be calculated using the relation $T = \sqrt{E^*/a}$, where E^* is the excitation energy of the fissioning system at the saddle point ($E^* = E_{\text{c.m.}} + Q - B_f(l) - E_{\text{rot}}(l) - E_n$) and a is the level density parameter, which is taken as $A_{\text{CN}}/10$, where A_{CN} is the mass of the fissioning CN. Here, $E_{\text{c.m.}} + Q$ is the excitation energy of the CN, $B_f(l)$ and $E_{\text{rot}}(l)$ are the l-dependent fission barrier and rotational energy, respectively. E_n is the reduction in the excitation energy of the CN by evaporating neutrons that is taken from the literature [19], while I_{eff}, B_f, and E_{rot} were obtained by using a rotating finite-range model [20]. The fitting parameters ν and μ are calculated for the reaction $^{16}O + ^{197}Au$, and the same parameters are used for the other

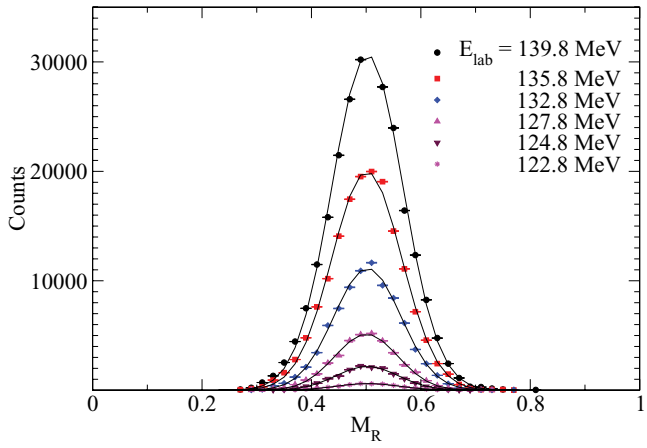

FIG. 6. (Color online) Mass ratio distributions for the reaction $^{27}Al + ^{186}W$ at different bombarding energies along with the Gaussian fits.

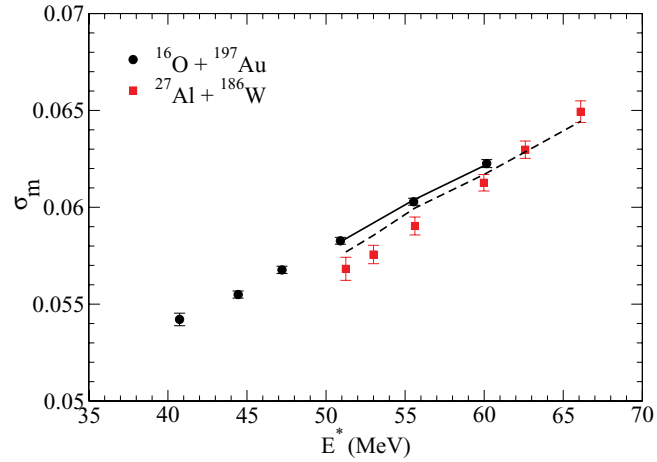

FIG. 7. (Color online) The standard deviation of the Gaussian fit to the mass distributions as a function of excitation energy along with the calculated values, using parameters obtained by fitting the $^{16}O + ^{197}Au$ reaction.

system to calculate the mass variance. If $^{27}Al + ^{186}W$ is also evolve through true CN fission, the same parameters deduced for $^{16}O + ^{197}Au$ ($\nu = 2.33 \times 10^{-3} \pm 0.0254 \times 10^{-3}$ and $\mu = 4.43 \times 10^{-7} \pm 0.0571 \times 10^{-7}$) have to reproduce the experimental fission mass widths. To rule out any contribution from lower $\langle l^2\rangle$ distributions that may result in ER formations that compete with the fission cross sections, we consider only the energy points $E^* > 50$ MeV to obtain the fits. The standard deviations of the Gaussian fits to the mass ratio distributions are plotted as a function of excitation energy in Fig. 7. It can be clearly observed that both the systems show an increase in σ_M with increasing excitation energy of the CN. The increasing trend in σ_M is as expected, with increasing excitation energy the mean square angular momentum and temperature of the fissioning CN will also increase and that will lead to an increase in the fission mass ratio distribution. It is also observed that the same values of ν and μ reproduce the experimental mass widths for the reaction $^{27}Al + ^{186}W$, indicating that reactions in both the systems proceed by the CN mechanism as shown in Fig. 7. Also a weak dependence of l^2 on σ_M^2 is observed for the present systems as shown in Table II. Figure 8 shows the ratio between experimental to calculated variances of the fission mass distributions as a function of CN excitation energy. It can be observed that the ratio of experimental to calculated fission mass widths is nearly equal to one, thereby indicating that both the reactions proceed through the CN mechanism. The experimental and calculated values of mass variance are given in Table II.

The dynamical evolution of the fused system in the presence of non-compound nuclear processes depends on the entrance channel parameters, such as the charge product (Z_pZ_t) of the colliding nuclei and deformation [4–7]. For deformed nuclei, the contact configuration of the interacting systems at the capture may influence the reaction dynamics significantly leading to QF. It is reported that the onset of QF starts at around $Z_pZ_t = 711$ for CN Ra [3], 888 for CN Rn [12], and around 1000 for CN Po [1]. The $^{27}Al + ^{186}W$ system has a Z_pZ_t value of 962, which is very similar to the above

TABLE II. Experimental and calculated values of mass variance for the two systems (for $^{16}O + ^{197}Au$ energy points $E^* > 50$ MeV are considered, as mentioned in the text).

Systems studied	E^* (MeV)	$\langle l^2 \rangle$	Temperature	$\sigma^2_{m\,\mathrm{exp}}$	$\sigma^2_{m\,\mathrm{cal}}$
$^{16}O + ^{197}Au$	50.82	424	1.376	0.00339	0.00339
	55.44	624	1.448	0.00363	0.00365
	60.07	817	1.507	0.00388	0.00387
$^{27}Al + ^{186}W$	51.08	218	1.389	0.00323	0.00333
	52.82	330	1.410	0.00331	0.00343
	55.44	503	1.449	0.00341	0.00359
	59.81	651	1.511	0.00375	0.00381
	62.43	804	1.545	0.00397	0.00395
	65.92	1034	1.587	0.00422	0.00415

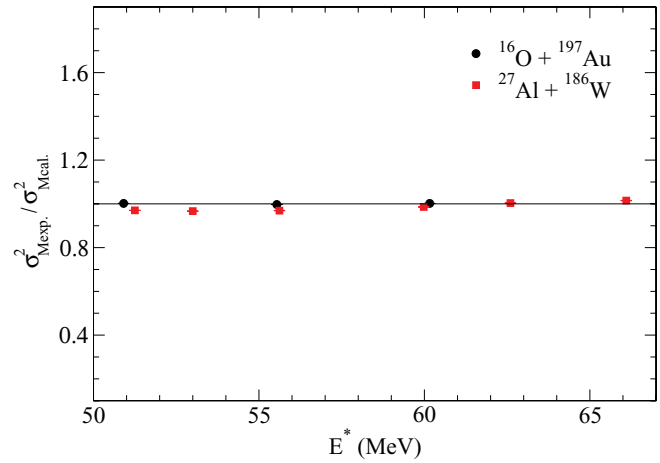

FIG. 8. (Color online) Ratio between experimental and calculated variance of mass distribution for the reactions $^{16}O + ^{197}Au$ (circles) and $^{27}Al + ^{186}W$ (squares) as a function of excitation energy.

reported systems, and the fissility of the present reaction is much higher than the fissilities of the previously reported compound systems Po and Rn. However, in the present work, there was no evidence of QF. Although, it is possible that the target deformation may favor the QF process in the $^{27}Al + ^{186}W$ reaction, when the projectile interacts with the tips of the deformed ^{186}W target nuclei leading to disintegration as QF before approaching the shape of CN. However, the experimental results suggest that the evolution of the fission process for the $^{27}Al + ^{186}W$ system in the multidimensional potential surface does not favor the occurrence of QF. Rather, it leads to complete mass equilibration when compared to reactions with actinide targets, where the fission barrier (B_f) values are small. Moreover, the occurrence of QF depends on the interaction time of the target and projectile combination with respect to the characteristic relaxation time of various degrees of freedom such as mass and K equilibration, as the dinuclear system goes to fission [5]. Further the interaction time between the projectile and target combination depends on entrance channel parameters such as the mass asymmetry of the interacting partners, deformation, shell effects, and the values of Z_pZ_t of the colliding nuclei. For the present systems studied, it seems that the interaction time is long enough for complete mass equilibration, as there is no evidence of QF. The absence of QF may also be due to the closed shell structure of the CN ($N = 126$). It was previously reported that at closed or nearly closed neutron shells there is some evidence of fission hindrance with increasing excitation energy [21]. There is some evidence of mass as well as K equilibration for the reactions with Z_pZ_t values around 900 [1,22]. The present study leads to the conclusion that for every compound system there exists a Z_pZ_t value for the onset of QF. The onset of QF needs to be further investigated by using a more symmetric combination forming the same CN to understand the factors that influence QF in less fissile systems.

IV. SUMMARY AND CONCLUSIONS

Mass angle correlations have been measured for the systems $^{16}O + ^{197}Au$ and $^{27}Al + ^{186}W$ leading to the same CN ^{213}Fr around the Coulomb barrier energies. Systematic analysis based on dependence of mass variance on temperature and angular momentum for both the systems indicates that the two systems evolve through true CN to fission. Earlier, for the compound nuclei Ra and Rn, the onset of QF was reported to be observed at much lesser values of Z_pZ_t. Even though the present system $^{27}Al + ^{186}W$ has $Z_pZ_t \sim 1000$, the onset of QF has not been not observed. This anomaly needs to be further investigated using more symmetric systems.

ACKNOWLEDGMENTS

The authors acknowledge the support of the Pelletron staff of IUAC, New Delhi, India, for providing excellent quality beams throughout the experiment. One of the authors (SA) is thankful to IUAC and CSIR, New Delhi, for providing financial assistance to the present research work. SM thanks DAE-BRNS, Mumbai, for providing financial assistance through a major research project. We also thank Dr. H. J. Wollersheim and R. Kumar for providing ^{186}W targets. We acknowledge the support received at various stages from target and vacuum laboratories at IUAC.

[1] R. Rafiei, R. G. Thomas, D. J. Hinde, M. Dasgupta, C. R. Morton, L. R. Gasques, M. L. Brown, and M. D. Rodriguez, Phys. Rev. C **77**, 024606 (2008).

[2] R. G. Thomas, D. J. Hinde, D. Duniec, F. Zenke, M. Dasgupta, M. L. Brown, M. Evers, L. R. Gasques, M. D. Rodriguez, and A. Diaz-Torres, Phys. Rev. C **77**, 034610 (2008).

[3] A. C. Berriman, D. J. Hinde, M. Dasgupta, C. R. Morton, R. D. Butt, and J. O. Newton, Nature (London) **413**, 144 (2001).

[4] W. J. Swiatecki, Phys. Scr. **24**, 113 (1981).

[5] J. P. Blocki, H. Feldmeier, and W. J. Swiatecki, Nucl. Phys. A **459**, 145 (1986).

[6] D. J. Hinde, M. Dasgupta, J. R. Leigh, J. P. Lestone, J. C. Mein, C. R. Morton, J. O. Newton, and H. Timmers, Phys. Rev. Lett. **74**, 1295 (1995).
[7] A. Yu. Chizhov *et al.*, Phys. Rev. C **67**, 011603(R) (2003).
[8] B. B. Back, R. R. Betts, J. E. Gindler, B. D. Wilkins, S. Saini, M. B. Tsang, C. K. Gelbke, W. G. Lynch, M. A. McMahan, and P. A. Baisden, Phys. Rev. C **32**, 195 (1985).
[9] V. S. Ramamurthy and S. S. Kapoor, Phys. Rev. Lett. **54**, 178 (1985).
[10] R. N. Sagaidak *et al.*, Phys. Rev. C **68**, 014603 (2003).
[11] R. Tripathi, K. Sudarshan, S. Sodaye, A. V. R. Reddy, K. Mahata, and A. Goswami, Phys. Rev. C **71**, 044616 (2005).
[12] E. Prasad *et al.*, Phys. Rev. C **81**, 054608 (2010).
[13] S. Appannababu *et al.*, Phys. Rev. C **80**, 024603 (2009).
[14] A. Jhingan, P. Sugathan, K. S. Golda, R. P. Singh, T. Varughese, Hardev Singh, B. R. Behera, and S. K. Mandal, Rev. Sci. Instrum. **80**, 123502 (2009).
[15] R. K. Choudhury *et al.*, Phys. Rev. C **60**, 054609 (1999).
[16] G. N. Knyazheva *et al.*, Phys. Rev. C **75**, 064602 (2007).
[17] K. Hagino, N. Rowley, and A. T. Kruppa, Comput. Phys. Commun. **123**, 143 (1999).
[18] S. Raman, At. Data Nucl. Data Tables **36**, 1 (1987).
[19] A. Saxena, A. Chatterjee, R. K. Choudhury, S. S. Kapoor, and D. M. Nadkarni, Phys. Rev. C **49**, 932 (1994).
[20] A. J. Sierk, Phys. Rev. C **33**, 2039 (1986).
[21] B. B. Back, D. J. Blumenthal, C. N. Davids, D. J. Henderson, R. Hermann, D. J. Hofman, C. L. Jiang, H. T. Penttila, and A. H. Wuosmaa, Phys. Rev. C **60**, 044602 (1999).
[22] R. Tripathi, K. Sudarshan, S. K. Sharma, K. Ramachandran, A. V. R. Reddy, P. K. Pujari, and A. Goswami, Phys. Rev. C **79**, 064607 (2009).